

## Beam energy dependence of the anisotropic flow coefficients $v_n$

---

**Niseem Magdy\*** (For the STAR Collaboration)

*Department of Chemistry, Stony Brook University, Stony Brook, NY, 11794-3400, USA*

*E-mail: niseemm@gmail.com*

Recent STAR measurements of the anisotropic flow coefficients,  $v_n$ , are presented for Au+Au collisions spanning the beam energy range  $\sqrt{s_{NN}} = 7.7 - 200$  GeV. The measurements indicate dependences on harmonic number,  $n$ , transverse momentum ( $p_T$ ), pseudorapidity ( $\eta$ ), collision centrality (cent) and beam energy ( $\sqrt{s_{NN}}$ ) which could serve as important constraints to test different initial-state models and to aid precision extraction of the temperature dependence of the specific shear viscosity.

*Critical Point and Onset of Deconfinement*

*, 7-11 August 2017*

*The Wang Center, Stony Brook University, Stony Brook, NY*

---

\*Speaker.

## 1. Introduction

A major goal of the heavy-ion experimental program at the Relativistic Heavy Ion Collider (RHIC) is to study the properties of the strongly interacting quark-gluon plasma (QGP) created in ion-ion collisions. Recently, many studies have emphasized the use of anisotropic flow measurements to study the transport properties of the QGP [1–7]. An important question in many of these studies has been the role of initial-state fluctuations and their influence on the uncertainties associated with the extraction of  $\eta/s$  for the QGP [8, 9]. This work presents new measurements for the anisotropic flow coefficients,  $v_{n>1}$ , and the rapidity-even dipolar flow coefficient,  $v_1^{even}$ , with an eye toward developing new constraints which could aid a distinction between different initial-state models and hence, facilitate a more precise extraction of the specific shear viscosity  $\eta/s$  [10, 11].

Anisotropic flow is characterized by the Fourier coefficients,  $v_n$ , obtained from a Fourier expansion of the azimuthal angle ( $\phi$ ) distribution of the particles emitted in the collisions [12]:

$$\frac{dN}{d\phi} \propto 1 + 2 \sum_{n=1} v_n \cos(n(\phi - \Psi_n)), \quad (1.1)$$

where  $\Psi_n$  represents the azimuthal angle of the  $n^{\text{th}}$ -order event plane; the coefficients,  $v_1$ ,  $v_2$  and  $v_3$  are commonly called directed, elliptic, and triangular flow, respectively. The flow coefficients,  $v_n$ , are related to the two-particle Fourier coefficients,  $v_{n,n}$ , as:

$$v_{n,n}(p_T^a, p_T^b) = v_n(p_T^a)v_n(p_T^b) + \delta_{\text{NF}}, \quad (1.2)$$

where a and b are particles selected with  $p_T^a$  and  $p_T^b$  respectively, and  $\delta_{\text{NF}}$  is a so-called non-flow (NF) term, which includes possible short-range contributions from resonance decays, Bose-Einstein correlations and near-side jets, and long-range contributions from the global momentum conservation (GMC) [13–15]. The short-range contributions can be reduced by employing a pseudorapidity gap,  $\Delta\eta$ . However, the effects of GMC must be explicitly considered. For the current analysis, a simultaneous fitting procedure, outlined below, was used to account for GMC.

## 2. Measurements

The correlation function technique was used to measure the two-particle  $\Delta\phi$  correlations:

$$C_r(\Delta\phi, \Delta\eta) = \frac{(dN/d\Delta\phi)_{\text{same}}}{(dN/d\Delta\phi)_{\text{mixed}}}, \quad (2.1)$$

where  $(dN/d\Delta\phi)_{\text{same}}$  represent the normalized azimuthal distribution of particle pairs from the same event and  $(dN/d\Delta\phi)_{\text{mixed}}$  represents the normalized azimuthal distribution for particle pairs in which each member is selected from a different event but with a similar classification for the collision vertex location, centrality, etc. The pseudorapidity requirement  $|\Delta\eta| > 0.7$  was also imposed on track pairs to minimize non-flow contributions associated with the short-range correlations.

The two-particle Fourier coefficients,  $v_{n,n}$ , are obtained from the correlation function as:

$$v_{n,n} = \frac{\sum_{\Delta\phi} C_r(\Delta\phi, \Delta\eta) \cos(n\Delta\phi)}{\sum_{\Delta\phi} C_r(\Delta\phi, \Delta\eta)}, \quad (2.2)$$

and then used to extract  $v_1^{even}$  via a simultaneous fit of  $v_{1,1}$  as a function of  $p_T^b$ , for several selections of  $p_T^a$  with Eq. 1.2:

$$v_{1,1}(p_T^a, p_T^b) = v_1^{even}(p_T^a)v_1^{even}(p_T^b) - Cp_T^ap_T^b. \quad (2.3)$$

Here,  $C \propto 1/(\langle Mult \rangle \langle p_T^2 \rangle)$  takes into account the non-flow correlations induced by a global momentum conservation [15, 16] and  $\langle Mult \rangle$  is the corrected mean multiplicity. For a given centrality selection, the left hand side of Eq. 2.3 represents the  $N \times N$  matrix which we fit with the right hand side using  $N + 1$  parameters;  $N$  values of  $v_1^{even}(p_T)$  and one additional parameter  $C$ , accounting for the momentum conservation [17].

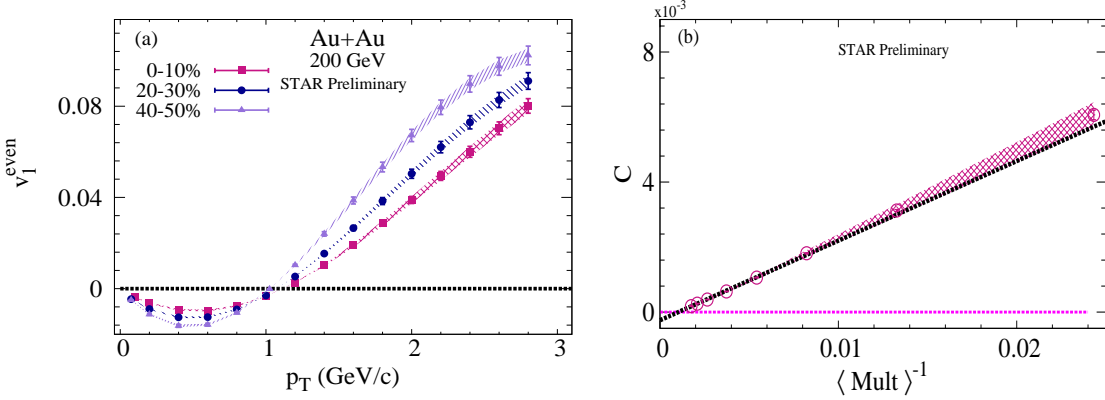


**Figure 1:** (a) The extracted values of  $v_1^{even}$  vs.  $p_T$  for Au+Au collisions at  $\sqrt{s_{NN}} = 200$  GeV. (b) A representative set of the associated values of  $C$  vs.  $\langle Mult \rangle^{-1}$  from the same fits. The shaded bands represent the systematic uncertainty.

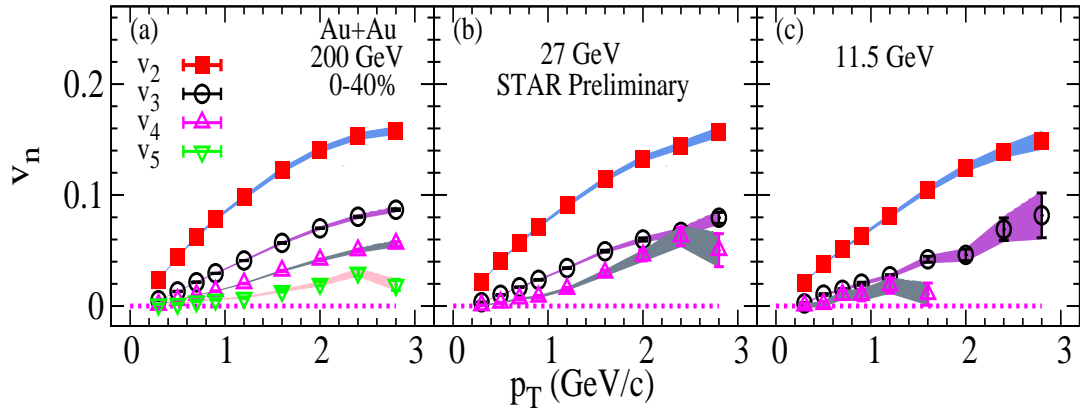
### 3. Results

Representative results for  $v_1^{even}$  and  $v_{n \geq 2}$  for Au+Au collisions at several different collision energies are summarized in Figs. 1, 2, 3, 4 and 5.

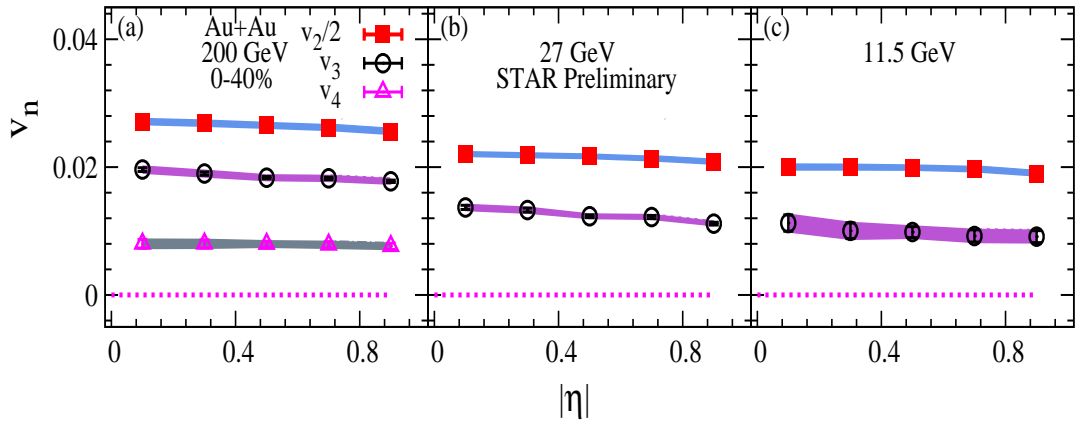
The values of  $v_1^{even}(p_T)$  extracted for different centrality selections (0-10%, 20-30% and 40-50%) are shown in Fig. 1(a). They indicate the characteristic pattern of a change from negative  $v_1^{even}(p_T)$  at low  $p_T$  to positive  $v_1^{even}(p_T)$  for  $p_T > 1$  GeV/c. They also show the expected increase of  $v_1^{even}$  as collisions become more peripheral, in line with the expected centrality dependence of the dipole asymmetry  $\varepsilon_1$ , where  $\varepsilon_1 \equiv |(r^3 e^{i\phi})|/r^3$  [18, 19]. Fig. 1(b) shows the results for the associated momentum conservation coefficients,  $C$ ; they indicate the expected linear dependence on  $\langle Mult \rangle^{-1}$ .

Figure 2 and 3 show  $p_T$  and  $\eta$  differential  $v_{n \geq 2}$  measurements for the centrality selection 0-40%, for a representative set of beam energies. Fig. 2 indicates a sizable dependence of the magnitude of  $v_n$  on  $p_T$  and the harmonic number,  $n$ , with similar trends for each beam energy. Figure 3 shows a similarly strong  $n$  dependence for  $v_{n \geq 2}$  but with a much weaker  $\eta$  dependence.

The centrality dependence of  $v_{n \geq 2}$  is shown in Fig. 4 for the same representative set of beam energies. They indicate a weak centrality dependence for the higher harmonics, which all decrease



**Figure 2:** Examples of  $v_n(p_T)$  as a function of  $p_T$  for charged particles in 0-40% central Au+Au collisions. The shaded bands represent the systematic uncertainty.



**Figure 3:** Examples of  $v_n(|\eta|)$  as a function of  $|\eta|$  for charged particles in 0-40% central Au+Au collisions. The shaded bands represent the systematic uncertainty.

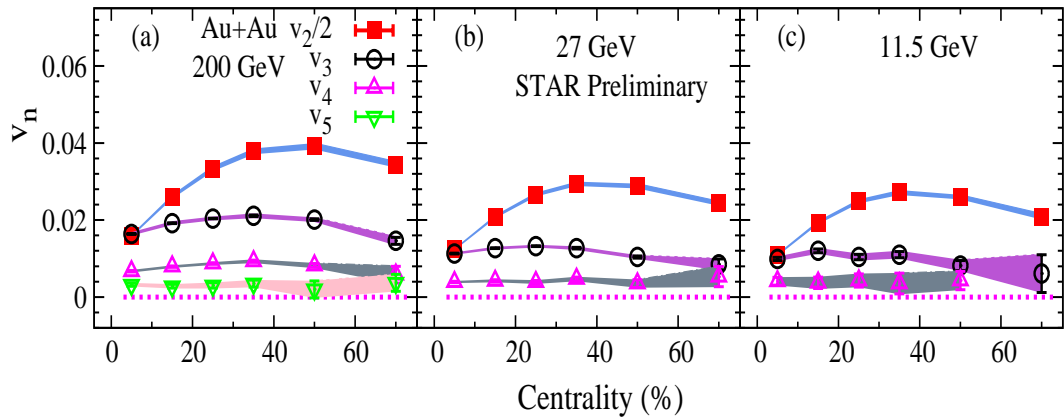


**Figure 4:** Examples of  $v_n(\text{Centrality}\%)$  as a function of Au+Au collision centrality for charged particles with  $0.2 < p_T < 4$  GeV/c. The shaded bands represent the systematic uncertainty.

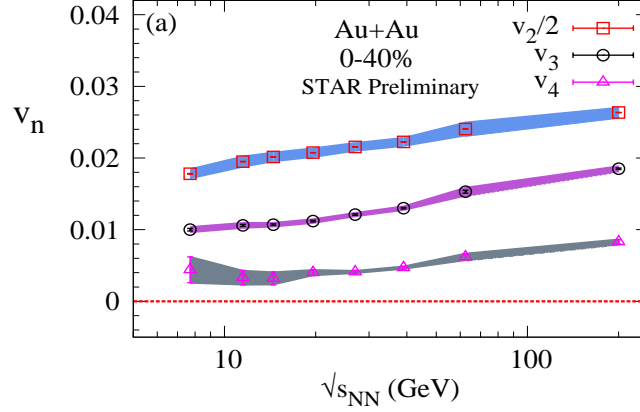


**Figure 5:** Examples of  $v_n(\sqrt{s_{NN}})$  for charged particles with  $0.2 < p_T < 4$  GeV/c and 0-40% central Au+Au collisions. The shaded bands represent the systematic uncertainty.

with decreasing values of  $\sqrt{s_{NN}}$ . These patterns may be related to the detailed dependence of the viscous effects in the created medium, which serve to attenuate the magnitude of  $v_n$ .

Figure 5 shows the excitation functions for the  $p_T$ -integrated  $v_{2,3,4}$  for 0–40% central Au+Au collisions. They indicate an essentially monotonic trend for  $v_2$ ,  $v_3$  and  $v_4$  with  $\sqrt{s_{NN}}$ , as might be expected for a temperature increase with  $\sqrt{s_{NN}}$ .

#### 4. Conclusion

In summary, we have performed a comprehensive set of STAR anisotropic flow measurements for Au+Au collisions at  $\sqrt{s_{NN}} = 7.7$ -200 GeV. The measurements use the two-particle correlation method to extract the Fourier coefficients,  $v_{n>1}$ , and the rapidity-even dipolar flow coefficient,  $v_1^{even}$ . The rapidity-even dipolar flow measurements indicate the characteristic patterns of an evolution from negative  $v_1^{even}(p_T)$  for  $p_T < 1$  GeV/c to positive  $v_1^{even}(p_T)$  for  $p_T > 1$  GeV/c, expected when initial-state geometric fluctuations act along with the hydrodynamic-like expansion to generate rapidity-even dipolar flow. The  $v_{n>1}$  measurements indicate a rich set of dependences on harmonic number  $n$ ,  $p_T$ ,  $|\eta|$  and centrality for versus the beam energy. These new measurements may provide additional constraints to test different initial-state models, and to aid precision extraction of the temperature dependence of the specific shear viscosity.

#### Acknowledgments

This research is supported by the US Department of Energy under contract DE-FG02-87ER40331.

#### References

- [1] D. Teaney, *The Effects of viscosity on spectra, elliptic flow, and HBT radii*, *Phys.Rev.* **C68** (2003) 034913, [nucl-th/0301099].
- [2] R. A. Lacey and A. Taranenko, *What do elliptic flow measurements tell us about the matter created in the little bang at RHIC?*, *PoS CFRNC2006* (2006) 021, [nucl-ex/0610029].

- [3] B. Schenke, S. Jeon and C. Gale, *Anisotropic flow in  $\sqrt{s} = 2.76$  TeV Pb+Pb collisions at the LHC*, *Phys.Lett.* **B702** (2011) 59–63, [1102.0575].
- [4] H. Song, S. A. Bass and U. Heinz, *Elliptic flow in 200 A GeV Au+Au collisions and 2.76 A TeV Pb+Pb collisions: insights from viscous hydrodynamics + hadron cascade hybrid model*, *Phys.Rev.* **C83** (2011) 054912, [1103.2380].
- [5] H. Niemi, G. Denicol, P. Huovinen, E. Molnar and D. Rischke, *Influence of a temperature-dependent shear viscosity on the azimuthal asymmetries of transverse momentum spectra in ultrarelativistic heavy-ion collisions*, *Phys.Rev.* **C86** (2012) 014909, [1203.2452].
- [6] G.-Y. Qin, H. Petersen, S. A. Bass and B. Muller, *Translation of collision geometry fluctuations into momentum anisotropies in relativistic heavy-ion collisions*, *Phys.Rev.* **C82** (2010) 064903, [1009.1847].
- [7] STAR collaboration, N. Magdy, *Viscous Damping of Anisotropic Flow in 7.7–200 GeV Au+Au Collisions*, *J. Phys. Conf. Ser.* **779** (2017) 012060.
- [8] B. Alver and G. Roland, *Collision geometry fluctuations and triangular flow in heavy-ion collisions*, *Phys. Rev.* **C81** (2010) 054905, [1003.0194].
- [9] R. A. Lacey, D. Reynolds, A. Taranenko, N. N. Ajitanand, J. M. Alexander, F.-H. Liu et al., *Acoustic scaling of anisotropic flow in shape-engineered events: implications for extraction of the specific shear viscosity of the quark gluon plasma*, *J. Phys.* **G43** (2016) 10LT01, [1311.1728].
- [10] J. Auvinen, I. Karpenko, J. E. Bernhard and S. A. Bass, *Investigating the collision energy dependence of  $\eta/s$  in RHIC beam energy scan using Bayesian statistics*, 1706.03666.
- [11] J. Auvinen, I. Karpenko, J. E. Bernhard and S. A. Bass, *Revealing the collision energy dependence of  $\eta/s$  in RHIC-BES Au+Au collisions using Bayesian statistics*, *Nucl. Phys.* **A967** (2017) 784–787, [1704.04643].
- [12] A. M. Poskanzer and S. A. Voloshin, *Methods for analyzing anisotropic flow in relativistic nuclear collisions*, *Phys. Rev.* **C58** (1998) 1671–1678, [nucl-ex/9805001].
- [13] R. A. Lacey, *The Role of elliptic flow correlations in the discovery of the sQGP at RHIC*, *Nucl. Phys.* **A774** (2006) 199–214, [nucl-ex/0510029].
- [14] N. Borghini, P. M. Dinh and J.-Y. Ollitrault, *Are flow measurements at SPS reliable?*, *Phys. Rev.* **C62** (2000) 034902, [nucl-th/0004026].
- [15] ATLAS collaboration, G. Aad et al., *Measurement of the azimuthal anisotropy for charged particle production in  $\sqrt{s_{NN}} = 2.76$  TeV lead-lead collisions with the ATLAS detector*, *Phys. Rev.* **C86** (2012) 014907, [1203.3087].
- [16] E. Retinskaya, M. Luzum and J.-Y. Ollitrault, *Directed flow at midrapidity in  $\sqrt{s_{NN}} = 2.76$  TeV Pb+Pb collisions*, *Phys. Rev. Lett.* **108** (2012) 252302, [1203.0931].
- [17] J. Jia, S. K. Radhakrishnan and S. Mohapatra, *A study of the anisotropy associated with dipole asymmetry in heavy ion collisions*, *J. Phys.* **G40** (2013) 105108, [1203.3410].
- [18] D. Teaney and L. Yan, *Triangularity and Dipole Asymmetry in Heavy Ion Collisions*, *Phys. Rev.* **C83** (2011) 064904, [1010.1876].
- [19] P. Bozek, *Event-by-event viscous hydrodynamics for Cu+Au collisions at  $\sqrt{s_{NN}}=200$  GeV*, *Phys. Lett.* **B717** (2012) 287–290, [1208.1887].